

DNS of turbulent spray flame water droplet interaction using an Euler-Lagrange-Lagrange scheme

J. Hasslberger¹, R. Concetti¹, N. Chakraborty² and M. Klein¹

¹Institute of Applied Mathematics and Scientific Computing, Bundeswehr University Munich, Neubiberg, Germany

²School of Engineering, Newcastle University, Newcastle Upon Tyne, United Kingdom

1 Introduction

The manipulation of flames by water droplets has relevance in internal combustion engines (e.g. BMW M4 GTS engine, WaterBoost system by Bosch), gas turbines [1], and also in the context of fire suppression and explosion mitigation [2]. It is instructive to note that water stands out by a very high liquid-gas density ratio as well as the highest specific heat and latent heat of vaporization of all liquids (cf. Table 1).

In terms of the physical effects of water droplet flame interaction, the cooling effect due to droplet evaporation and the dilution effect due to reactants mass fraction reduction are to be considered. Note that the cooling, i.e. gas temperature reduction, occurs due to the phase change enthalpy sink and the mass source in the gaseous phase, i.e. gas density increase, under isobaric combustion conditions. The reductions of fuel and oxidizer concentration as well as temperature are directly affecting the local burning rate and thus flame speed. However, it has been shown [3] that the cooling effect outweighs the dilution effect for water droplet premixed flame interaction.

To complement the earlier findings, the focus of this study is placed on a comparison of water droplet addition for premixed and spray flames. Subjected to a constant water droplet stream from the inlet, different configurations of statistically planar turbulent n-heptane/air flames are investigated for this purpose by means of carrier-phase direct numerical simulation (DNS).

2 Computational method

The two-way coupled hybrid scheme (implemented in SENGAP+, a three-dimensional compressible DNS code [4]) is based on a 10th order finite difference discretization for the gas phase Eulerian representation and a Lagrangian point particle representation for both fuel droplets and water droplets. The relevant liquid properties of n-heptane fuel droplets and water droplets are summarized in Table 1. The gas-phase chemical reaction is described by a one-step irreversible Arrhenius-type ansatz [5] for the purpose of computational

Table 1: Liquid droplet properties of n-heptane and water

	n-heptane	water	Unit
Density	684.0	999.9	kg/m ³
Molecular mass	100.0	18.02	g/mol
Latent heat of vaporization (at boiling temperature)	315.0	2258.0	kJ/kg
Specific heat at constant pressure	2296.45	4181.0	J/kg/K

economy. This computational methodology has successfully been used in several earlier DNS studies on n-heptane spray flames (e.g. [6, 7]).

A canonical inflow-outflow configuration has been chosen with periodic boundaries in both lateral directions. Ensuring to resolve the thermal flame thickness as well as the Kolmogorov length scale, the rectangular simulation domain of size $30\delta_{st} \times 20\delta_{st} \times 20\delta_{st}$ has been discretized by $384 \times 256 \times 256$ grid points. The turbulent flow field following a Batchelor-Townsend energy spectrum is initially imposed throughout the domain and continuously maintained at the inlet. It is generated by a pseudo-spectral method and characterized by a turbulence intensity of $u'/S_L = 4$ and an integral turbulent length scale of $L_{11}/\delta_{st} = 2.5$, where S_L and δ_{st} are the burning velocity and the thermal flame thickness of the unstretched laminar stoichiometric premixed flame without water addition, respectively. Considering the fuel in liquid and gaseous phases, an overall equivalence ratio $\phi_{ov} = \phi_l + \phi_g$ of unity is maintained throughout the simulation. The overall water loading $Y_W = Y_W^l + Y_W^g = m_W/(m_0 + m_W)$, where m_0 is the initial unburned gas mass in the system before adding the liquid water droplets of mass m_W , accounts for the water mass fraction in both phases. This quantity is independent of the product water generated by the chemical reaction. The investigated value of $Y_W = 0.1$ lies in the technically relevant range and is also comparable to earlier experimental studies [1, 2]. Whereas the size of initially mono-disperse fuel droplets is $a_d/\delta_{st} = 0.04$, the size of initially mono-disperse water droplets is varied between $a_d/\delta_{st} = 0.02$ and 0.04 for constant $Y_W = 0.1$ – resulting in strong differences regarding the effect of water addition.

An impression of the problem setup can be obtained from Fig. 1. Unlike in unity Lewis number premixed flames (where $c = T$ holds), isosurfaces of reaction progress variable c and normalized temperature T are clearly non-conforming, which is mainly due to the heat sink associated to evaporating water droplets (see the localized dimples on the $T = 0.9$ isosurface). Also note that the highly volatile fuel droplets rarely reach the hot gas side of the flame, whereas the water droplets penetrate far into the post-flame region ($c = 1$) according to their low volatility, i.e. high latent heat of vaporization.

3 Results and discussion

Figure 2 shows the different structures of the premixed flame and spray flame with water addition, respectively. The temperature reduction effect due to water droplets can be seen for both types of flames, considering that $T = 1$ corresponds to the adiabatic flame temperature of the stoichiometric premixed flame without water addition. In the spray flame case, the temperature is additionally lowered because the partially premixed combustion takes place under fuel-lean conditions as can be seen from Fig. 5. The steam mass fraction Y_W^g exclusive of the product water in the flame region (enclosed by the white isolines) remains much smaller than the overall water loading Y_W irrespective of the type of flame. Hence, the dilution effect

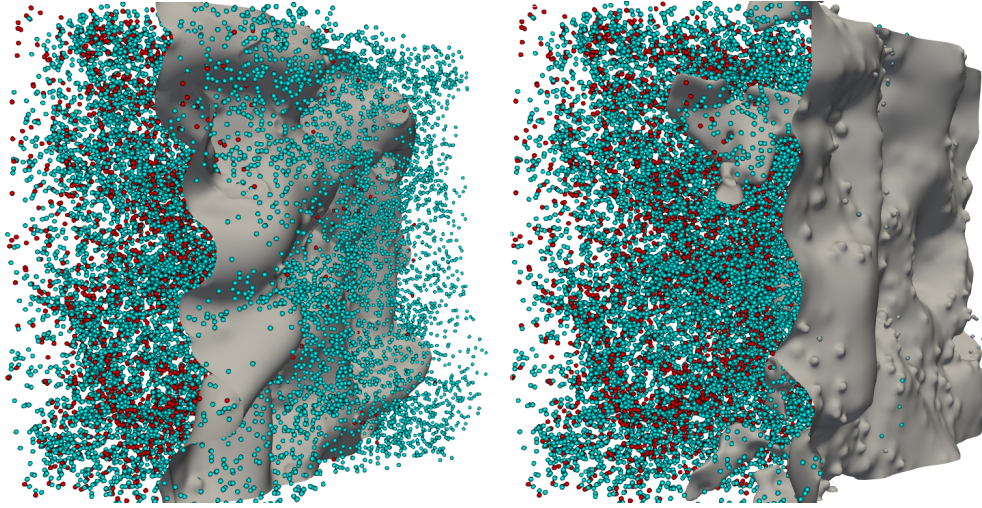


Figure 1: Isosurfaces of reaction progress variable $c = 0.9$ on the left and normalized temperature $T = 0.9$ on the right at $t/t_{chem} = 1.1$ for the spray flame case with water addition. Not-to-the-scale spheres indicate the fuel droplets (red) and water droplets (blue).

on in-flame characteristics is generally small while large steam mass fractions are observed in the post-flame region. However, the amount of steam within the spray flame is higher than in the premixed flame.

It is well-known that the evolution of turbulent burning velocity S_T and flame surface area A are strongly linked. To isolate the effects of fuel/water droplets and (turbulent) wrinkling on the flame, it is useful to examine the amount of burning per unit area of flame,

$$\Omega = \frac{\int_V \dot{\omega}_c dV}{\int_V |\nabla c| dV}. \quad (1)$$

Hence, deviations of the ratio

$$\frac{S_T/S_L}{A/A_\perp} = \frac{\Omega}{\rho_0 S_L} \quad (2)$$

from unity quantify the departure from the idealised premixed flame behaviour as postulated by Damköhler's first hypothesis. Note that $S_T = \int_V \dot{\omega}_c dV / (\rho_0 A_\perp)$ and the flame area projected onto the direction of mean flame propagation A_\perp is identical to the initial flame surface area A_0 for the statistically planar flame. Figure 3 demonstrates, firstly, the smaller values of Ω for the fuel-lean spray flame and, secondly, the consistent lowering of Ω through water droplet addition. The non-monotonic temporal evolution is a consequence of the underlying turbulent flow field.

In agreement with flame speed trends, as measured by Ω , inverse trends of the flame thickness can be observed in Fig. 4. In analogy to the thermal flame thickness, an alternative flame thickness based on the peak mean value of the surface density function (SDF), $|\nabla c|$, can be defined by

$$\delta_{SDF} = \frac{1}{\max(|\nabla c|)}, \quad (3)$$

where $\langle \cdot \rangle$ indicates conditional averaging upon reaction progress c . Normalization by the thermal flame thickness δ_{st} of the unstretched laminar stoichiometric premixed flame without water addition again facilitates the quantitative comparison with this idealized flame configuration. In terms of the effect of the water

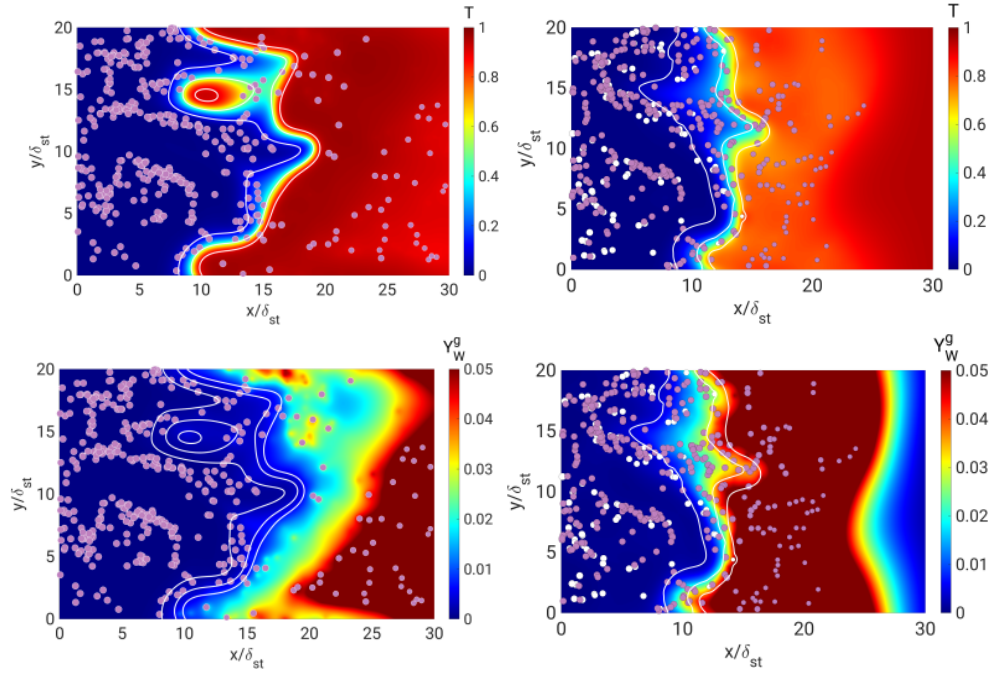


Figure 2: Mid-plane contours of normalized temperature T (top row) and steam mass fraction Y_W^g exclusive of the product water (bottom row) at $t/t_{chem} = 4.1$ for premixed fuel (left) and fuel spray (right). Not-to-the-scale dots indicate the fuel droplets (white) and water droplets (pink), both of initial size $a_d/\delta_{st} = 0.04$. White isolines represent $c = 0.1, 0.5, 0.9$, respectively.

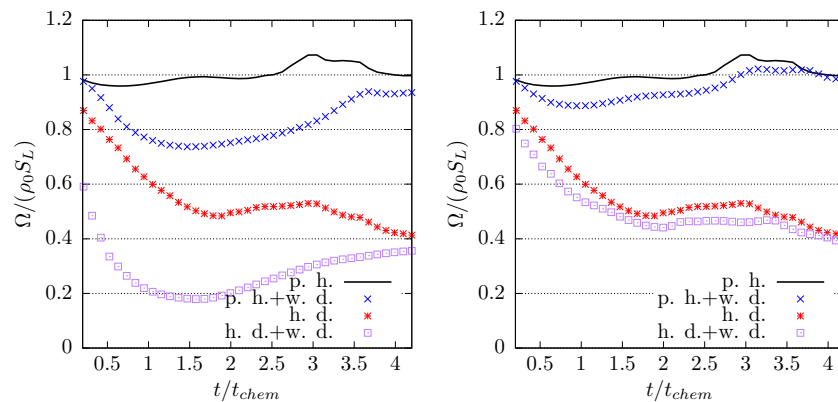


Figure 3: Temporal evolution of the normalized amount of burning per unit area of the flame Ω . Water droplets with initial $a_d/\delta_{st} = 0.02$ on the left and $a_d/\delta_{st} = 0.04$ on the right. The following abbreviations are used in all subsequent figures: premixed heptane (p.h.), heptane droplets (h.d.), water droplets (w.d.).

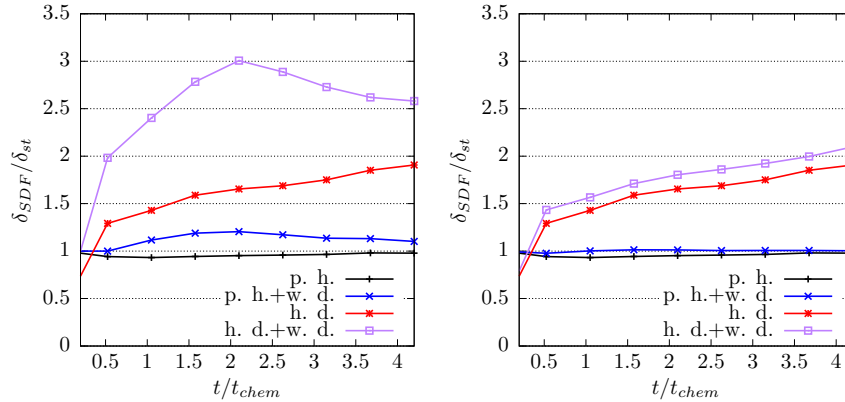


Figure 4: Temporal evolution of the normalized mean flame thickness δ_{SDF} based on the flame surface density function (SDF). Water droplets with initial $a_d/\delta_{st} = 0.02$ on the left and $a_d/\delta_{st} = 0.04$ on the right.

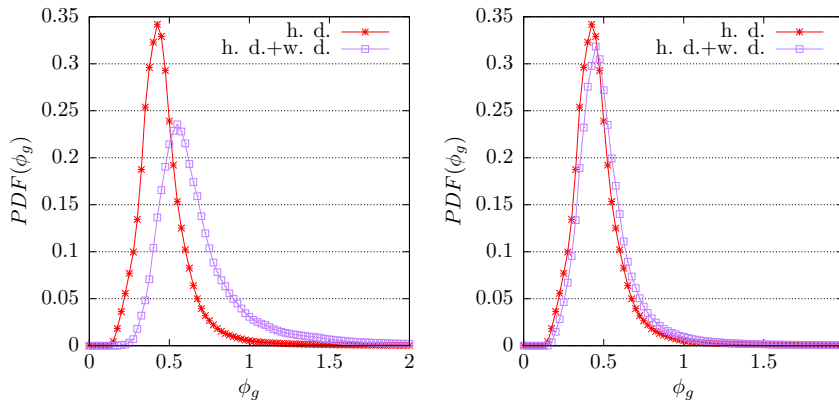


Figure 5: Probability density function of the gaseous equivalence ratio ϕ_g in the flame region ($0.1 < c < 0.9$) for the spray flame cases at $t/t_{chem} = 3$. Water droplets with initial $a_d/\delta_{st} = 0.02$ on the left and $a_d/\delta_{st} = 0.04$ on the right.

droplet size a_d/δ_{st} , a strong non-linear effect emerges as can be expected from the “diameter squared”-law governing evaporation. The smaller the water droplet size, the faster the droplet evaporation and the stronger the thickening of the flame.

Figure 5 finally shows the probability density function (PDF) of the gaseous equivalence ratio ϕ_g in the flame region, i.e. for $0.1 < c < 0.9$. Since the overall equivalence ratio $\phi_{ov} = \phi_l + \phi_g = 1$ is maintained during the spray flame simulations, the partially premixed combustion takes place under fuel-lean conditions. It is now interesting to see that water addition in the spray flame cases leads to relatively fuel-richer conditions. This is explained by the increased thickness of flames and thus longer residence time of fuel droplets within the flame, leaving more time for droplet evaporation. Also, via the cooling effect, the thermal expansion is attenuated which again affects the residence time of fuel droplets within the flame. Furthermore, the water addition enhances the mixture inhomogeneity as can be seen from the flattened, i.e. increased-width, PDF of the gaseous equivalence ratio.

4 Conclusions and outlook

An Euler-Lagrange-Lagrange scheme has been employed to study the impact of water droplet addition on statistically planar turbulent flames. It has been shown earlier [3] that the main effect on key flame characteristics, such as flame speed and flame thickness, is due to the heat sink associated to evaporating water droplets. However, water droplet addition influences spray combustion in a more intricate way than premixed combustion. Despite the steam-related dilution effect, the spray flame burns under fuel-richer conditions, i.e. higher gaseous equivalence ratio, at identical overall equivalence ratio. Due to the non-linear influence of droplet size on the evaporation law, considerable differences have been observed for water droplet sizes of $a_d/\delta_{st} = 0.04$ (moderate effect) and $a_d/\delta_{st} = 0.02$ (strong effect) at identical overall water loading.

Additional work (to be presented at the conference) will focus on the combustion mode analysis and also on the reaction zone structure in these spray flames. This is particularly important because of the coexistence of premixed and diffusive combustion due to mixture inhomogeneity in the spray flame cases considered here.

References

- [1] Lellek, S., Barfuß, C., & Sattelmayer, T. (2017). Experimental study of the interaction of water sprays with swirling premixed natural gas flames. *Journal of Engineering for Gas Turbines and Power*, 139(2).
- [2] Thomas, G. O. (2000). On the conditions required for explosion mitigation by water sprays. *Process Safety and Environmental Protection*, 78(5), 339-354.
- [3] Hasslberger, J., Ozel-Erol, G., Chakraborty, N., Klein, M., & Cant, S. (2021). Physical effects of water droplets interacting with turbulent premixed flames: A Direct Numerical Simulation analysis. *Combustion and Flame*, 229, 111404.
- [4] Jenkins, K. W., & Cant, R. S. (2002). Curvature effects on flame kernels in a turbulent environment. *Proceedings of the Combustion Institute*, 29(2), 2023-2029.
- [5] Fernandez-Tarrazo, E., Sanchez, A. L., Linan, A., & Williams, F. A. (2006). A simple one-step chemistry model for partially premixed hydrocarbon combustion. *Combustion and Flame*, 147(1-2), 32-38.
- [6] Ozel Erol, G., Hasslberger, J., Klein, M., & Chakraborty, N. (2018). A direct numerical simulation analysis of spherically expanding turbulent flames in fuel droplet-mists for an overall equivalence ratio of unity. *Physics of Fluids*, 30(8), 086104.
- [7] Ozel Erol, G., Hasslberger, J., Klein, M., & Chakraborty, N. (2019). A direct numerical simulation investigation of spherically expanding flames propagating in fuel droplet-mists for different droplet diameters and overall equivalence ratios. *Combustion Science and Technology*, 191(5-6), 833-867.